
CMS Conference Report

30 April 1998

The CMS Silicon Tracker Detector: an overview of the R&D current status

A. Santocchia¹³, S. Albergo⁴, M. Angarano², P. Azzi¹², E. Babucci¹³, N. Bacchetta¹², A. Bader², G. Bagliesi¹⁴, P. Bartalini¹³, A. Basti¹⁴, U. Biggeri⁶, G.M. Bilei¹³, D. Bisello¹², D. Boemi⁴, F. Bosi¹⁴, L. Borrello¹⁴, C. Bozzi¹⁴, H. Breuker⁷, M. Bruzzi⁶, A. Candelori¹², A. Caner⁷, R. Castaldi¹⁴, A. Castro¹², E. Catacchini⁶, B. Checcucci¹³, P. Ciampolini¹³, C. Civinini⁶, J. Connotte¹, D. Creanza², R. D'Alessandro⁶, M. Da Rold¹², M. de Palma², R. Dell'Orso¹⁴, R. Della Marina¹⁵, C. Eklund⁸, A. Elliott-Peisert⁷, L. Fiore², E. Focardi⁶, M. French⁵, K. Freudenreich¹⁵, A. Giassi¹⁴, A. Giraldo¹², B. Glessing⁷, W.H. Gu¹, G. Hall¹⁰, R. Hammerstrom⁷, J. Hrubec¹⁶, M. Huhtinen⁷, V. Karimäki⁸, M. Krammer¹⁶, P. Lariccia¹³, M. Loreti¹², K. Luebelsmeyer¹, W. Lustermann¹⁵, G. Maggi², M. Mannelli⁷, G. Mantovani¹³, A. Marchioro⁷, G. Martignon¹², B. Mc Evoy¹⁰, M. Meschini⁶, A. Messineo¹⁴, S. My², A. Paccagnella¹², F. Palla¹⁴, D. Pandoulas¹, G. Parrini⁶, D. Passeri¹³, M. Pieri⁶, S. Piperov³, R. Potenza⁴, F. Raffaelli¹⁴, G. Raso², M. Raymond¹⁰, B. Schmitt⁷, G. Selvaggi², L. Servoli¹³, G. Sguazzoni¹⁴, R. Siedling¹, L. Silvestris^{2,7}, K. Skog⁸, A. Starodumov¹⁴, I. Stavitsky¹², G. Stefanini⁷, P. Tempesta², G. Tonelli¹⁴, A. Tricomi⁴, T. Tuuva⁹, C. Vannini¹⁴, P.G. Verdini¹⁴, G. Viertel¹⁵, Z. Xie¹⁴, Y. Wang¹³, S. Watts¹¹, B. Wittmer¹

-
- ¹) I. Physikalisches Institut, RWTH, Aachen, Germany
²) Università di Bari e Sez. dell'INFN, Bari, Italy
³) Humboldt University, Berlin, Germany
⁴) Università di Catania e Sez. dell'INFN, Catania, Italy
⁵) RAL, Didcot, United Kingdom
⁶) Università di Firenze e Sez. dell'INFN, Firenze, Italy
⁷) CERN, European Laboratory for Particle Physics, Geneva, Switzerland
⁸) Helsinki Institute of Physics, Helsinki, Finland
⁹) University of Oulu, Kemi, Finland
¹⁰) Imperial College, University of London, London, United Kingdom
¹¹) Brunel University, Middlesex, United Kingdom
¹²) Università di Padova e Sez. dell'INFN, Padova, Italy
¹³) Università di Perugia e Sez. dell'INFN, Perugia, Italy
¹⁴) Università di Pisa e Sez. dell'INFN, Pisa, Italy
¹⁵) Laboratory for High Energy Physics, ETH-Z, Zürich, Switzerland
¹⁶) Institut für Hochenergiephysik der OeAW, Wien, Austria

Abstract

The paper describes the Silicon Tracking System of the Compact Muon Solenoid (CMS) and reviews the most recent results of the R&D activity on radiation resistant microstrip silicon detectors. The Silicon Tracker of CMS consists of 5 layers of microstrip detectors in the barrel and 10 disks on either side of the end-cap region. The detectors of the innermost layers (22.5 cm radial distance from the beam pipe) are required to operate up to an integrated fluence of 1.6×10^{14} 1-MeV-equivalent neutrons per cm^2 . The results, obtained with single-sided prototypes irradiated with a neutron fluence up to 2×10^{14} n/ cm^2 in terms of signal-to-noise ratio, efficiency and spatial resolution are described. We also show a comparison between device simulations, laboratory measurements and experimental results. Lastly we describe the complex system prototypes which have been recently built to address the system aspects of such a large silicon tracker.

Presented at *Hiroshima@Melbourne*, Melbourne, December 10, 1997

Submitted to *Nuclear Instruments and Method*

1 Introduction

The Compact Muon Solenoid (CMS) [1] is a general purpose detector designed to find new physics by identifying muons, electrons and photons and measuring their properties over a large energy range at LHC. The CMS detector (Fig. 1) consists of a Muon Detection System, a large (13 m long, 6 m in diameter), 4 Tesla superconducting solenoid, Hadronic and Electromagnetic Calorimeters and a Central Tracking System. The CMS Tracker has been designed to reconstruct high p_T tracks with high efficiency over the pseudo-rapidity range $|\eta| < 2.5$ and a momentum resolution $\delta p_T/p_T = 0.15 p_T$ (TeV/c).

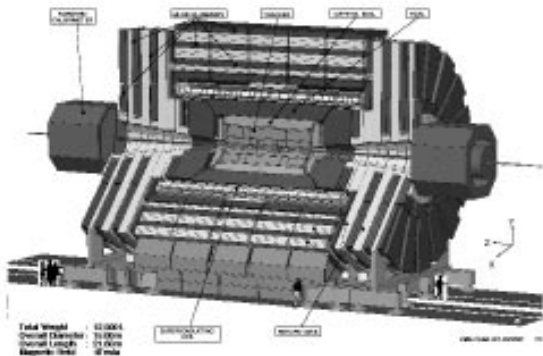


Figure 1: 3D view of the CMS detector

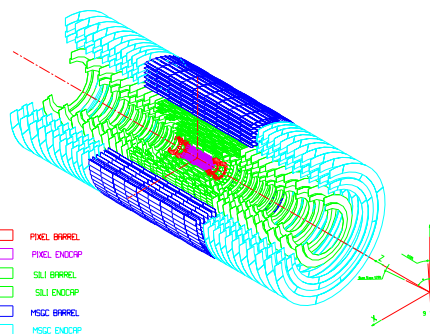


Figure 2: General layout of the CMS Central Tracker

The tracker (Fig. 2) is a 5.9 m long cylinder with 1.3 m radius and consists of 3 different subsystems: the Silicon Pixel Detector, the Silicon Strip Detector and the MicroStrip Gas Chambers.

The paper describes the main features of the CMS Silicon Tracker discussing in detail the long term survival after heavy irradiation.

It has been estimated that, in 10 years of LHC running, the most irradiated silicon strip detectors of CMS will be subjected to an average fluence of 1.6×10^{14} 1-MeV-equivalent neutrons per cm^2 . This value has been considered as design value for the radiation resistance of the full system.

2 The Silicon Tracker

The Silicon Tracker of CMS is subdivided in a barrel and an end-cap system. In the barrel, the radial region between 22 and 63.5 cm from the beam line and $|z| \leq 87$ cm will be instrumented with 5 layers of silicon detectors. The two inner layers and the outer one will be equipped with double-sided detector modules while only single-sided modules will be used in the intermediate layers. To maintain a high level of modularity, each cylindrical layer will be made of two independent carbon fiber (CF) shells. Fig. 3 shows one supporting structure of the barrel detector with cooling pipes and cables. A mini-endcap part, which will contain three small disks on each side, will also be included in the barrel system to complement the first two barrel layers with wedge-shaped detectors. This particular geometry will reduce the overall number of modules while recovering the detector performance for very inclined tracks.

The end-cap region will be equipped with 10 disks on each side. The z position of the disks has been optimized to guarantee full coverage and an efficient track reconstruction in the region $1.2 \leq |\eta| \leq 2.5$. To minimize the number of silicon wafers needed, 3 different sets of disks will be used, with the radius of the inner active ring varying from 22 cm to 38.5 cm, while the outer radius will be always 61 cm.

The total area of silicon sensors will be about 70 m^2 and $\approx 5 \times 10^6$ read-out channels will be instrumented. A description of the read-out system can be found in reference [2].

The precision required in the hit position measurement is $20 \mu\text{m}$ in the r - ϕ plane and better than $500 \mu\text{m}$ in the z coordinate. Table 1 resumes the main parameters of the Silicon Tracker.

Standard n -type, $300 \mu\text{m}$ thick (resistivity $\geq 2 \text{ K}\Omega \cdot \text{cm}$) silicon wafers will be used as starting material. Our choice for radiation resistant technology is based on standard p^+ implantation, integrated AC coupling capacitors and poly-silicon bias resistors [3]. A structure of multiple guard-rings is also foreseen around the active area. The

Table 1: Silicon Tracker parameters (L1-L5 are the 5 layers of the Barrel, M1-M2 and R1-R4 are the rings installed respectively in the Mini-Endcaps and in the Endcaps. The mean pitch is quoted. SS stands for Single-Sided and DS for Double-Sided.)

	Barrel					Mini Endcaps		Endcaps			
	L1	L2	L3	L4	L5	M1	M2	R1	R2	R3	R4
$R_{in} (cm)$	217	304.5	391.5	479	566	218	285	218	285	390	484
$R_{out} (cm)$	249	336.5	423.5	511	598	295	354	295	386	499	608
Readout	DS	DS	SS	SS	DS	DS	DS	DS	SS	SS	DS
$N_{ch}(\phi)$	1024	768	768	512	512	768	768	1024	768	512	512
Pitch (ϕ) (μm)	61	81	81	122	122	60	74	60	78	103	127
$N_{ch}(\text{stereo})$	512	512	-	-	256	512	512	512	-	-	256
Pitch (stereo) (μm)	122	122	-	-	244	89	111	89	-	-	254

innermost ring is used to bias the implants and the outer ones to collect the edge contribution of the leakage current and to properly shape the field lines for better breakdown performance.

The choice of AC coupled, poly-biased, single-sided p^+ on n -bulk devices as baseline sensors allows very high voltage operation, achievable in simplified technology. The radiation resistance of these devices has been proven to be above the expected fluence in CMS. They are relatively simple and low cost devices since their production is compatible with standard micro-electronics technology. For the same reason they can be produced in large quantities with high yield by several manufacturers.

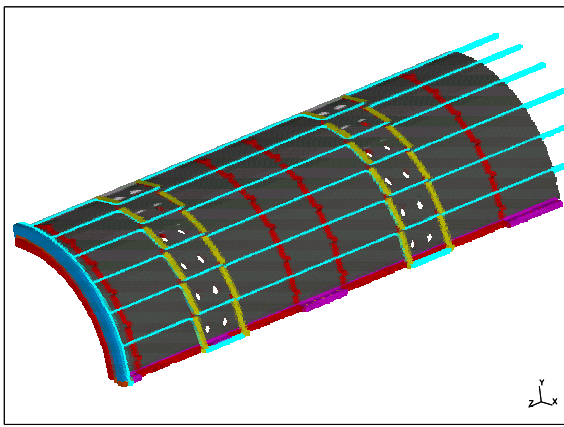


Figure 3: The supporting structure of the barrel detector

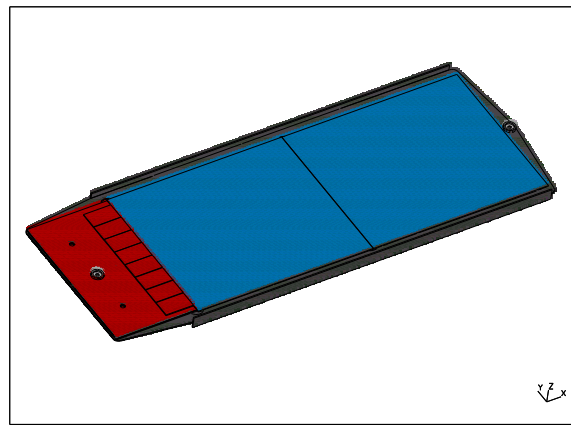


Figure 4: Perspective view of a single-sided barrel module

For the double-sided layers we plan to use two single-sided back-to-back sensors, one of which will have small angle stereo strips. To avoid dead regions the use of double metal connections is envisaged. This choice simplifies high voltage operation since the electronics can be operated without an offset ground which is necessary when truly double-sided devices are used.

The basic detection units, both in the barrel and in the end-cap region, will be detector modules similar to the one shown in Fig. 4. Two single-sided silicon wafers ($6.4 \times 6.4 \text{ cm}^2$) are daisy chained together, for a total strip length of about 12.5 cm, connected to a readout unit and glued onto a carbon fiber frame. The CF structure has been designed to allow an adequate heat transfer from the sensors and from the readout electronics to the cooling pipes integrated in the supporting structure.

3 The R&D Status

An extensive simulation work has been carried out to evaluate the performance of heavily irradiated devices. The main limiting factor for the lifetime of the silicon detectors will be the increase of the depletion voltage [4] [5] caused by the changes of the effective doping concentration in the bulk. This phenomenon has been carefully evaluated using a general purpose device simulator, the HFIELDS program [6].

To study the charge collection mechanism in arbitrarily “damaged” devices, the program has been slightly modified

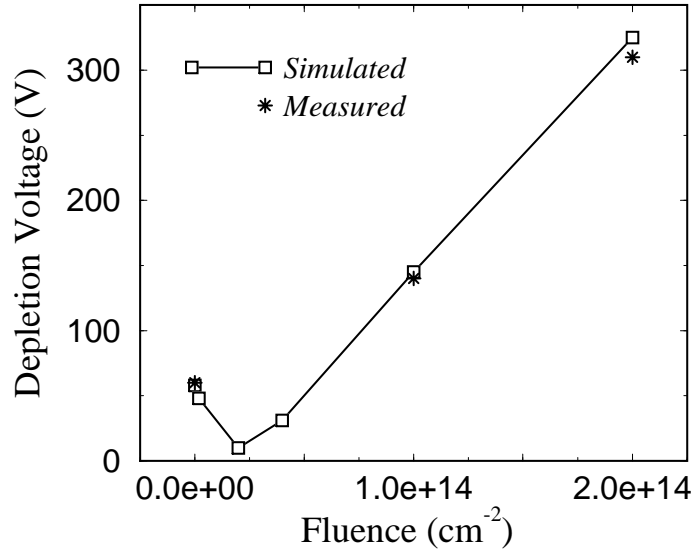


Figure 5: Comparison between estimated depletion voltage vs. fluence and experimental data Initial resistivity of silicon was about $5 \text{ K}\Omega\cdot\text{cm}$

and a transient-analysis mode has been widely used [7]. First, non-damaged devices have been simulated: an AC analysis has been carried out and a good agreement has been found with laboratory data. Then, in order to calibrate the model, the inversion point was tuned to the specific device under study. Among the most relevant parameters, the depletion voltage can be extracted from the AC analysis and thus correlated to the radiation suffered by the device.

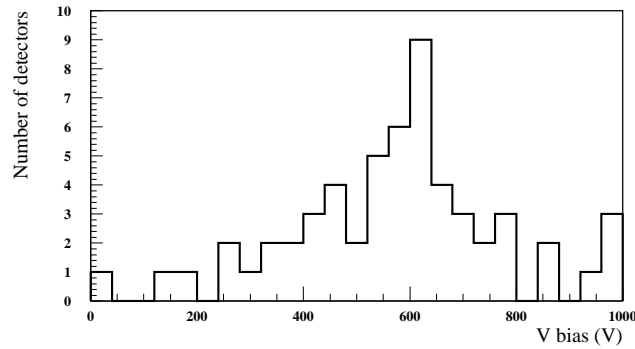


Figure 6: Distribution of breakdown voltage values for full side detectors ($6.4 \times 6.4 \text{ cm}^2$) produced by CSEM

The comparison between the expected depletion voltage and the results of laboratory measurements on irradiated detectors is shown in Fig. 5. After $1.6 \times 10^{14} \text{ n/cm}^2$ we expect that the detectors of the innermost layers will reach a depletion voltage between 200 and 300 V. To fully collect the charge and to reduce the contribution to the noise due to the increased interstrip capacitance, we plan to overdeplete the most irradiated silicon modules. We therefore require to operate all detectors in a stable way at above 500 V bias both before and after radiation induced type inversion of the bulk.

To this purpose high voltage performances of several series of devices from different manufacturers have been carefully studied. As an example Fig. 6 shows the distribution of the breakdown voltage for a series of devices before irradiation. Most detectors fulfill the requirement of $V_{bkdn} \geq 500 \text{ V}$ and this fundamental characteristics is

also maintained after irradiation (see Fig. 7).

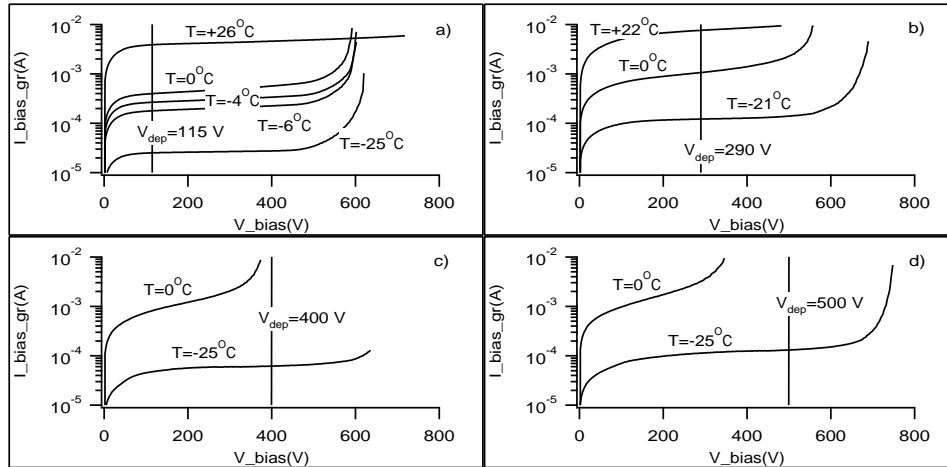


Figure 7: I-V-curves at different temperatures for neutron irradiated modules ($2 \times 6.4 \times 6.4 \text{ cm}^2$ detectors manufactured by CSEM). a) at $0.9 \times 10^{14} \text{ n/cm}^2$, b) at $1.8 \times 10^{14} \text{ n/cm}^2$, c) at $2.7 \times 10^{14} \text{ n/cm}^2$, d) at $3.6 \times 10^{14} \text{ n/cm}^2$

Further improvements of the breakdown performance are under study. Multiguard structures are one of the possible solutions to limit the occurrence of critical fields in the proximity of the junctions. They consist of a series of concentric floating guard rings placed around the detector's active area. The optimization process implies taking into account all the effects of irradiation. Ionizing particles produce surface damage with resulting increase of the accumulation layer and narrowing of the depletion region. As a consequence, a decrease of the breakdown voltage may occur. Promising results have been achieved on test structures featuring multiple thin p^+ rings surrounding the active area [8] [9]. The optimization process is still under study and new structures are under process. Irradiation tests will be soon performed to test the radiation hardness at higher fluences.

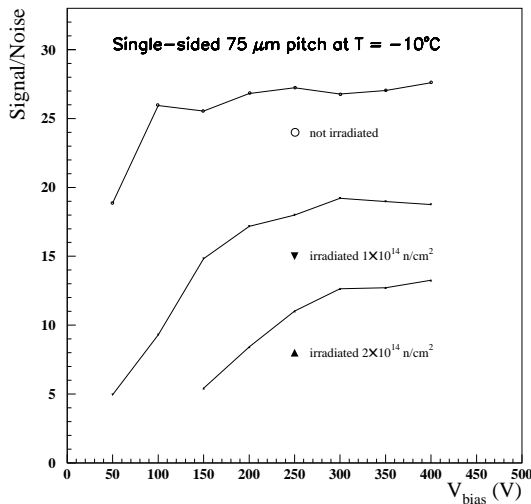


Figure 8: Signal-to-noise ratio as a function of V_{bias} for detector modules (11.5 cm strip length) at different fluences.

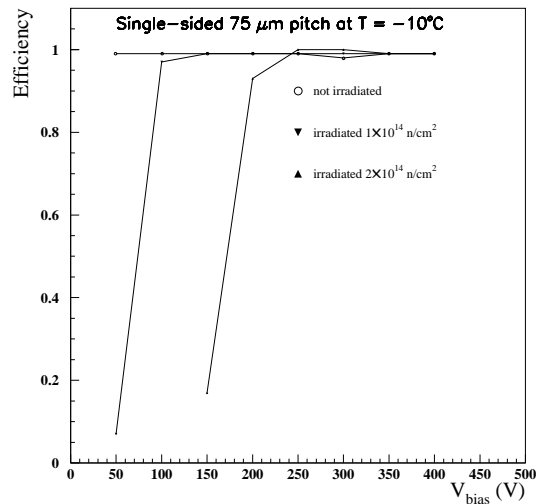


Figure 9: Hit efficiency vs. V_{bias} for different fluences

Several beam tests have been carried out in order to check carefully the performance of the devices in terms of signal-to-noise ratio, efficiency and space resolution under different conditions of bias voltage, temperature

and radiation damage. As an example we report on a set of $75\ \mu\text{m}$ pitch detectors which have been irradiated ($T=0^\circ\text{C}$, $V_{bias}=2V_{dep}$) with fluences of 1.0×10^{14} and 2.0×10^{14} n/cm^2 . All the devices have been stored at low temperature after irradiation to prevent reverse annealing effects and have been operated at $\approx -10^\circ\text{C}$ to avoid the thermal runaway phenomenon. Detector modules have been fabricated by coupling together pairs of these devices for a total strip length of 11.5 cm. Analogue amplifiers (PREMUX [10]) with peak mode readout and 50 ns shaping time, based on a similar input stage that is used in the final front-end chip, were used as readout electronics.

Fig. 8 shows a signal-to-noise ratio for the most irradiated detector of about 14. The detection efficiency after irradiation has been carefully evaluated. Fig. 9 shows the hit efficiency as a function of the bias voltage for different irradiation fluences. After 2.0×10^{14} n/cm^2 , detectors operated at $T=-10^\circ\text{C}$ reach full efficiency ($\approx 99\%$) at a bias voltage of $\approx 300\text{V}$. For what concerns the spatial resolution, we observe that it does not depend substantially on the fluence and bias voltage (Fig. 10). From the residual distribution for the $75\ \mu\text{m}$ pitch detectors we extract a spatial resolution of about $21\ \mu\text{m}$.

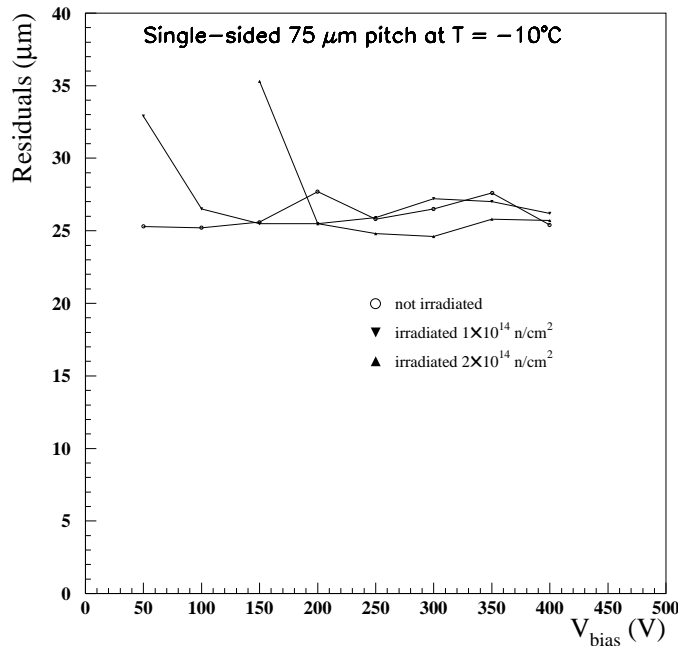


Figure 10: Width of the residual distribution for irradiated detector modules as a function of V_{bias}

4 Prototype Construction

During 1996 and 1997 an intense program has been carried out in order to demonstrate the capability of building our detector according to the complex requirements. The main issues that drove our design and the choice of materials used in the silicon tracker were the following: high mechanical precision of construction and stability during operation are needed to exploit the high accuracy of the silicon detectors; efficient cooling to operate the silicon devices at about -10°C is mandatory in order to limit the effect of radiation damage on silicon detectors; low density material is highly desirable to minimize the impact on the performances of the electromagnetic calorimeter surrounding the tracker; simple and standardized assembly procedures must be foreseen to allow reliable and precise construction of several thousand modules in a number of different production centers; lastly, all the materials employed should exhibit excellent radiation tolerance to maintain their properties in the high radiation environment of LHC.

Following the original technical proposal [1], a complete barrel wheel has been fully equipped with 15 real and 97 dummy modules (designed to dissipate the same amount of power as the real ones). Tests of alignment, stability, assembly and cooling have been performed to investigate the feasibility of the overall project. Fig. 11 shows the fully assembled wheel.

A complete end-cap disk, with a carbon fiber support structure fully equipped with 6 working modules and 30

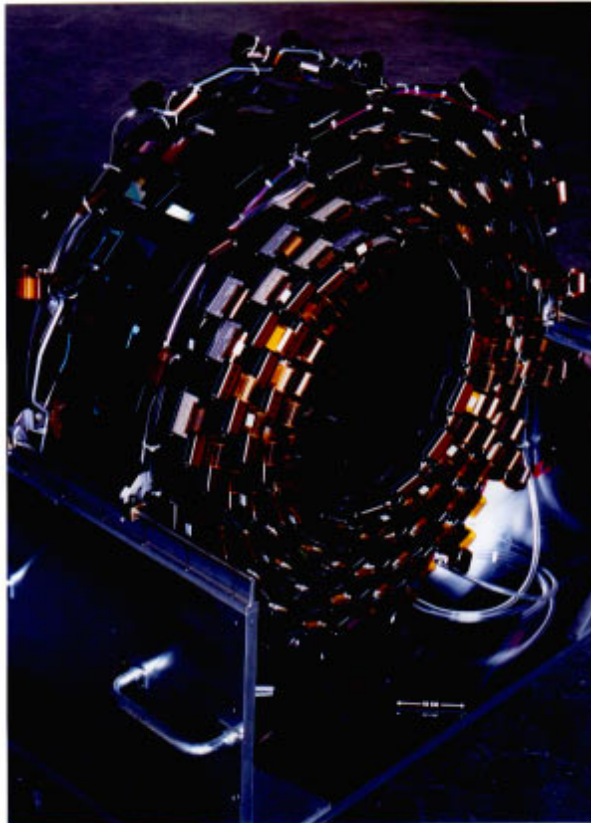


Figure 11: The fully instrumented Silicon Barrel Wheel

dummy modules has also been built.

The experience gained during this phase makes us confident that we shall be able to construct the CMS silicon tracker according to the specifications. For most of the problems and difficulties so far encountered we have already found satisfactory solutions, while for others we have identified a series of options which are being studied in order to identify the optimal choice.

5 Conclusion

The solutions chosen for the CMS Silicon Tracker appear well suited for operating the detector for ten years at LHC. The radiation damage effects are well understood and the optimization work done in the past few years make us confident that the single-sided p^+ on n technology is an appropriate choice. Full size prototypes of the barrel and of the end-cap sectors have been successfully produced. The Technical Design Report for the CMS Silicon Tracker is well under way to be delivered by April 1998.

References

- [1] *CMS Technical Proposal*, CERN/LHCC 94-38, 15 Dec. 1994
- [2] G. Hall and G. Stefanini *The CMS tracker readout System*, CMS-TN/94-137
- [3] G. Tonelli et al., *Double-sided radiation resistant microstrip detectors: technology and results* Nucl. Instr. and Meth. A377, pp. 422, 1996.
- [4] J. Matthews et. al. *Bulk radiation damage in silicon detectors and implications for LHC experiments* Nucl. Instr. and Meth. A381, pp. 338-348, 1996.
- [5] C. Leroy, M. Glaser, E.H.M. Heijne, P. Jarron, F. Lemeilleur, J. Rioux, C. Soave, I. Trigger, *Study of the electrical properties and charge collection of silicon detectors under neutron, proton and gamma irradiations* Nucl. Instr. and Meth. A360, pp. 458-462, 1995.

- [6] G. Bacarani, M. Rudan, R. Guerrieri and P. Ciampolini *Physical Models for Numerical device simulation* Process and Device Modeling, W.L. Engl cd., North Holland, Amsterdam pp 107-159, 1986
- [7] D. Passeri, M. Baroncini, P. Ciampolini, G.M. Bilei, A. Santocchia and B. Checcucci *TCAD-Based Analysis of Radiation-Hardness in Silicon Detectors*, IEEE Trans. Nucl. Sci. 45 (3), 1998
- [8] M. Da Rold et al., *Multiguard structures for high voltage operation of radiation damaged silicon detectors*, presented at the “3rd International Conference on Large Scale Applications and Radiation Hardness of Semiconductor Detectors”, to be published on IL NUOVO CIMENTO.
- [9] N. Bacchetta et al., *High voltage operation of silicon devices for LHC experiments* presented at the 7th Pisa Meeting, to be published on *Nucl. Instr. And Meth. in Phys. Res. A*.
- [10] L. L. Jones *PreMux128 User Manual*